



Temperature-dependent efficiency droop in AlGaIn epitaxial layers and quantum wells

J. Mickevičius, J. Jurkevičius, A. Kadys, G. Tamulaitis, M. Shur, M. Shatalov, J. Yang, and R. Gaska

Citation: *AIP Advances* **6**, 045212 (2016); doi: 10.1063/1.4947574

View online: <http://dx.doi.org/10.1063/1.4947574>

View Table of Contents: <http://scitation.aip.org/content/aip/journal/adva/6/4?ver=pdfcov>

Published by the [AIP Publishing](#)

Articles you may be interested in

[Deep ultraviolet photopumped stimulated emission from partially relaxed AlGaIn multiple quantum well heterostructures grown on sapphire substrates](#)

J. Vac. Sci. Technol. B **32**, 061204 (2014); 10.1116/1.4898694

[Correlation between carrier localization and efficiency droop in AlGaIn epilayers](#)

Appl. Phys. Lett. **103**, 011906 (2013); 10.1063/1.4813259

[Internal quantum efficiency in AlGaIn with strong carrier localization](#)

Appl. Phys. Lett. **101**, 211902 (2012); 10.1063/1.4767657

[Deep-ultraviolet emission of AlGaIn/AlN quantum wells on bulk AlN](#)

Appl. Phys. Lett. **81**, 4658 (2002); 10.1063/1.1524034

[Al concentration control of epitaxial AlGaIn alloys and interface control of GaN/AlGaIn quantum well structures](#)

J. Appl. Phys. **87**, 172 (2000); 10.1063/1.371840

A promotional banner for AIP Applied Physics Reviews. It features a blue background with a glowing light effect. On the left, there is a small image of a journal cover titled 'AIP Applied Physics Reviews' showing a diagram of a quantum well structure. The main text reads 'NEW Special Topic Sections' in large white letters. Below this, it says 'NOW ONLINE' in yellow, followed by 'Lithium Niobate Properties and Applications: Reviews of Emerging Trends' in white. The AIP Applied Physics Reviews logo is in the bottom right corner.

NEW Special Topic Sections

NOW ONLINE
Lithium Niobate Properties and Applications:
Reviews of Emerging Trends

AIP Applied Physics Reviews

Temperature-dependent efficiency droop in AlGaIn epitaxial layers and quantum wells

J. Mickevičius,^{1,a} J. Jurkevičius,¹ A. Kadys,¹ G. Tamulaitis,¹ M. Shur,²
 M. Shatalov,³ J. Yang,³ and R. Gaska³

¹Semiconductor Physics Department and Institute of Applied Research, Vilnius University, Sauletekio 9-III, LT-10222, Vilnius, Lithuania

²Department of ECE and CIE, Rensselaer Polytechnic Institute, Troy, NY 12180, USA

³Sensor Electronic Technology, Inc., 1195 Atlas Road, Columbia, SC 29209, USA

(Received 8 September 2015; accepted 14 April 2016; published online 21 April 2016)

Luminescence efficiency droop has been studied in AlGaIn epitaxial layers and multiple quantum wells (MQWs) with different strength of carrier localization in a wide range of temperatures. It is shown that the dominant mechanism leading to droop, i.e., the efficiency reduction at high carrier densities, is determined by the carrier thermalization conditions and the ratio between carrier thermal energy and localization depth. The droop mechanisms, such as the occupation-enhanced redistribution of nonthermalized carriers, the enhancement of nonradiative recombination due to carrier delocalization, and excitation-enhanced carrier transport to extended defects or stimulated emission, are discussed. © 2016 Author(s). All article content, except where otherwise noted, is licensed under a Creative Commons Attribution 3.0 Unported License. [<http://dx.doi.org/10.1063/1.4947574>]

III-nitride-based light-emitting diodes (LEDs) suffer from the efficiency droop effect: their quantum efficiency peaks at low driving currents and decreases significantly at higher currents, which are desired for high-power applications like general lighting. Auger recombination,¹⁻⁴ carrier leakage,⁵⁻⁷ and loss mechanisms associated with reduced carrier localization or the saturation of localized states⁸⁻¹⁰ have been proposed as the main origin of the droop. The efficiency droop is observed not only at increasing current injection in complete device structures, but also in epilayers under increasing photoexcitation. Thus, the carrier leakage⁵⁻⁷ cannot be considered as a single mechanism of the efficiency droop, since it is not expected under photoexcitation. The Auger recombination has been studied theoretically³ and was observed experimentally^{1,4} only in InGaIn structures. It is expected to be less pronounced in AlGaIn due to the anticipated reduction of Auger coefficient, both direct and phonon- or impurity-assisted, with increasing band gap.^{11,12}

On the other hand, the connection between carrier localization and efficiency droop has been demonstrated in InGaIn quantum well structures,^{9,13,14} AlGaIn epilayers,¹⁵ and AlGaIn quantum wells.¹⁶ Recently, we proposed the ratio $k_B T / \sigma$ between the carrier thermal energy $k_B T$ and localization parameter σ (i.e. the dispersion of the depth of potential fluctuations) as the figure of merit determining the prevailing efficiency droop mechanism in AlGaIn MQWs.¹⁶ We also demonstrated the significance of the redistribution of nonthermalized carriers within localized states on the efficiency droop at low temperatures in AlGaIn epilayers.¹⁷

In this paper, we expand on our recent work on temperature-dependent efficiency droop in AlGaIn materials. We show that, in addition to parameter $k_B T / \sigma$, carrier thermalization conditions are also important in determining the dominant efficiency droop mechanism.

A set of 30 samples consisting both of AlGaIn epilayers (labeled E1-E23) and MQWs (M1-M7) was selected for the study. All the samples were grown on c-plane sapphire substrates by using metalorganic chemical vapor deposition (MOCVD) and migration-enhanced MOCVD (MEMOCVD®) techniques. To cover a wider range in localization conditions, AlGaIn epilayers

^aElectronic mail: juras.mickevicius@ff.vu.lt



with aluminum content ranging from 17% to 78% were selected. The thickness of the epilayers varied between 1 and 2 μm . The Al molar fraction in the MQWs containing ten QWs ranged from 8 to 35%, while the well thickness was from 2.5 to 5.0 nm. The dislocation densities in the AlGaIn samples under study were estimated using the pits detected by atomic force microscopy and ranged between 5×10^8 and $1 \times 10^{10} \text{ cm}^{-3}$.

The carrier dynamics was studied by photoluminescence (PL) spectroscopy under quasi-steady-state conditions (with the pulse duration of 4 ns exceeding the carrier lifetime). The samples were excited using the 4th harmonic (266 nm) of the Q-switched YAG:Nd laser radiation and 213 nm line of the tunable-wavelength nanosecond laser (Ekspla NT342B). All the measurements were performed in a temperature range from 8 to 300 K using a closed-cycle helium cryostat. The luminescence emission of the samples was analyzed by a double monochromator (Jobin Yvon HRD-1) and detected by a UV-enhanced photomultiplier.

The temperature dependence of the PL band peak position was exploited to estimate the carrier localization parameters in the samples under study, as described in more details in Ref. 17. This approach enables us to estimate the standard deviation σ of the Gaussian distribution of the band gap fluctuations caused by the random fluctuations in aluminum content and/or QW width, and the parameter T_0 approximately corresponding to the temperature of the dip in the S-shaped dependence, i.e. the temperature above which the carrier thermalization becomes important.

We studied the efficiency droop correlation with the carrier localization conditions by measuring the excitation power density dependences of the spectrally-integrated PL efficiency in a wide temperature range. The typical dependences are provided in Fig. 1 for samples with weak [Fig. 1(a)] and strong [Fig. 1(b)] carrier localization. The efficiency droop onset was estimated from the experimental data as the excitation power density corresponding to the peak PL efficiency.

It is worth noting that, at any temperature, the droop onset is always higher in the samples with weaker carrier localization. Moreover, the droop onset increases with temperature more rapidly in the samples with weaker carrier localization. Since both temperature and localization parameter are important in determining the droop onset, we used the dimensionless parameter $k_B T / \sigma$ (the ratio of the thermal energy $k_B T$ with the dispersion of potential fluctuations σ), and plotted the

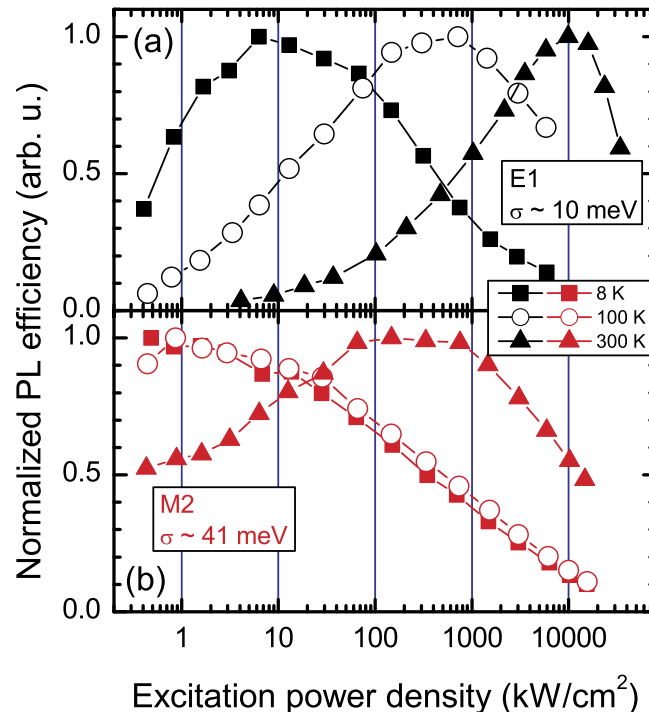


FIG. 1. Normalized PL efficiency dependences on excitation power density in AlGaIn samples with weak (a) and strong (b) carrier localization at 8 K (closed squares), 100 K (open circles) and 300 K (closed triangles).

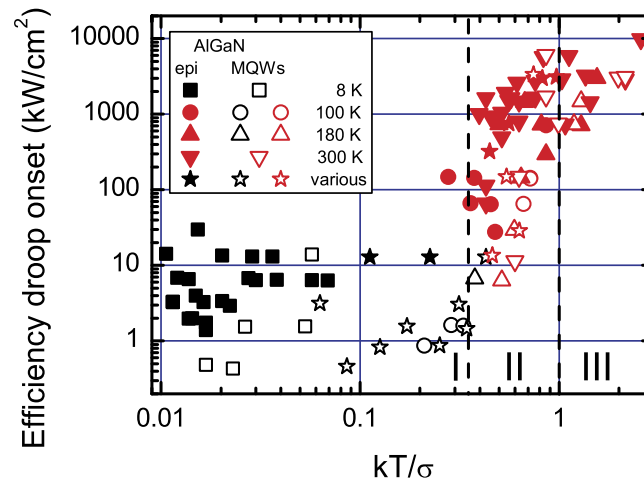


FIG. 2. Efficiency droop onset dependence on the ratio of thermal energy to localization parameter in AlGaIn epilayers and MQWs at various temperatures. Filled and open points indicate epilayers and MQWs, respectively. Black and red points correspond to the nonthermalized and thermalized distribution of carriers within localized states, respectively. Dashed lines separate regions corresponding to different efficiency droop mechanisms.

efficiency droop onset as a function of this parameter $k_B T/\sigma$ (see Fig. 2), similarly to what we did to reveal the droop mechanism in AlGaIn MQWs.¹⁶ Each point in Fig. 2 represents AlGaIn epilayer or MQW sample with specific σ value in the range from 10 to 65 meV and measured at a specific temperature in the range from 8 to 300 K. We indicate whether the temperature is above or below the thermalization temperature T_0 by plotting red or black points, respectively. We include the results obtained for both the epilayers and MQWs (filled and open points, respectively). As seen, the epilayers and MQWs exhibit similar trends. This is an indication that the carrier dynamics mainly depends on the thermalization and the $k_B T/\sigma$ ratio, independently of the potential fluctuation origin (which might be different in the epilayers and MQWs).

Despite the considerable scattering of points, which might be expected due to the different densities of nonradiative recombination centers in different samples, the plot might be divided into three regions. The first region covers all points corresponding to the nonthermalized state of the nonequilibrium carriers ($T < T_0$). This region is observed for $k_B T/\sigma < 0.35$ (region I in Fig. 2). The droop onset in this region is low, in the range from 1 to 10 kW/cm², and does not depend on $k_B T/\sigma$. As the carrier distribution becomes thermalized, the droop onset rapidly increases with parameter $k_B T/\sigma$ increasing in the range from 0.35 to 1 (region II in Fig. 2). Finally, the increase tends to saturation for $k_B T/\sigma > 1$. The last feature is consistent with our observations of the droop caused by stimulated emission in AlGaIn MQWs.¹⁶

The three regions observed in the dependence of droop onset versus $k_B T/\sigma$ are most likely related to the change in efficiency droop mechanism. The corresponding mechanisms are schematically shown in Fig. 3.

At temperatures below the thermalization temperature ($k_B T/\sigma < 0.35$, region I in Fig. 2), the carriers relax to the potential minima in the close vicinity of the carriers. Since the temperature is below the thermalization temperature T_0 , the carrier redistribution is weak, and they are not able to leave the local potential minima where they are captured to [Fig. 3(a)]. As the excitation is increased, the carriers (excitons) become more mobile since most of the nearest local minima are already occupied. Such occupation-enhanced carrier redistribution [see Fig. 3(b)] results in decreasing PL efficiency due to a higher probability of reaching nonradiative recombination centers.¹⁷

At elevated temperatures $T > T_0$ ($0.35 < k_B T/\sigma < 1$, region II in Fig. 2), the carriers are able to redistribute efficiently and become thermalized. As the excitation is increased, an increasing fraction of carriers becomes delocalized, while only the deeper localized states remain filled-in.^{15,16} The delocalized carriers can decrease the PL efficiency by the enhancement of nonradiative recombination as well as increase it due to bimolecular recombination,¹⁶ with the competition between

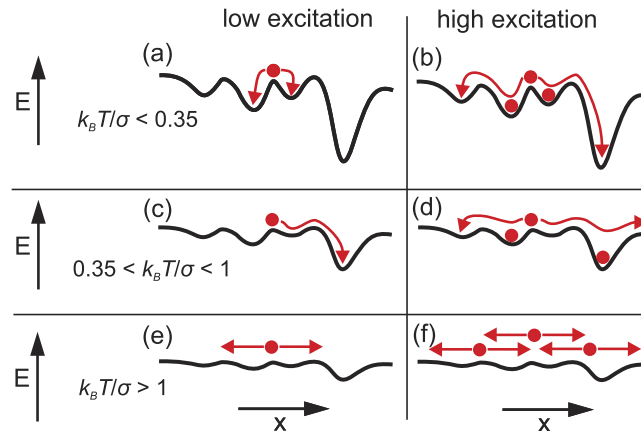


FIG. 3. Schematic diagrams of carrier transport at low (a), (c), (e) and high (b), (d), (f) excitations for the three regions of Fig. 2.

these two effects determined by the localization parameter σ . Due to the efficient thermal redistribution, higher carrier densities and, hence, excitation power densities are required to saturate the localized states and result in the efficiency droop via increased probability to reach the nonradiative recombination centers [see Fig. 3(d)].

At high temperatures and/or weak localization ($k_B T / \sigma > 1$, region III in Fig. 2), the carriers are predominantly free, since the thermal energy is higher than the localization parameter [Fig. 3(e) and 3(f)]. The efficiency droop onset in these samples is achieved at carrier densities in quite a wide range from 2×10^{19} to $2 \times 10^{20} \text{ cm}^{-3}$. This renders the Auger mechanism less probable as the droop origin, since Auger recombination might be expected to emerge at similar carrier densities in any sample of the same material. Furthermore, the stimulated emission threshold was shown to coincide with the droop onset in AlGaIn MQWs,¹⁶ and was identified as the droop origin. However, no stimulated emission has been observed at room temperature in the AlGaIn epilayers under study. One more droop mechanism might be related to excitation-dependent carrier transport: at low carrier densities, the nonradiative processes caused by point defects limit the carrier mobility. As the carrier density is increased, the point defects are saturated. Thus, the distance a carrier can move in real space during its lifetime is increased, and the nonradiative recombination at extended defects starts to dominate.^{14,18} Moreover, at high carrier densities, the carrier mobility is additionally enhanced due to carrier degeneracy.¹⁹ The carrier-density-enhanced recombination at the extended defects with distances between them larger than the average distance the carrier can travel during its lifetime at low temperature but comparable at room temperature is consistent with the supposed recombination at growth domains observed in AlGaIn epilayers by scanning near-field optical microscopy.^{20,21} During the growth, the adjacent islands coalesce into large grains. As a result of coalescence, the domain boundaries usually contain extended defects that form to accommodate the relative difference in crystal orientation among the islands.²² Thus, the onset of the droop caused by the fast nonradiative recombination at these boundaries does not strongly depend on $k_B T / \sigma$ but is rather determined by the grain size depending on lattice mismatch, buffer layer, and slightly on growth conditions.

In summary, the carrier thermalization conditions and the ratio $k_B T / \sigma$ between the carrier thermal energy $k_B T$ and localization parameter σ are the key parameters determining the dominant droop mechanism in AlGaIn epilayers and MQWs. For nonthermalized carriers ($k_B T / \sigma < 0.35$), the droop occurs due to occupation-enhanced redistribution of nonthermalized carriers. At elevated temperatures ($0.35 < k_B T / \sigma < 1$), the droop is caused by enhancement of the nonradiative recombination as the localized states are filled-in and an increasing fraction of carriers becomes delocalized. At high temperatures and/or weak localization ($k_B T / \sigma > 1$), the origin of the droop is stimulated emission in AlGaIn MQWs and excitation-enhanced carrier transport to extended defects in AlGaIn epilayers.

The work at VU was funded by the European Social Fund under the Global Grant measure project VP1-3.1-ŠMM-07-K-02-014. The work at RPI was supported primarily by the Engineering

Research Centers Program (ERC) of the National Science Foundation under NSF Cooperative Agreement No. EEC-0812056 and in part by New York State under NYSTAR contract C090145.

- ¹ J. Iveland, L. Martinelli, J. Peretti, J.S. Speck, and C. Weisbuch, *Phys. Rev. Lett.* **110**, 177406 (2013).
- ² Y.C. Shen, G.O. Mueller, S. Watanabe, N.F. Gardner, A. Munkholm, and M.R. Krames, *Appl. Phys. Lett.* **91**, 141101 (2007).
- ³ T. Sadi, P. Kivisaari, J. Oksanen, and J. Tulkki, *Appl. Phys. Lett.* **105**, 091106 (2014).
- ⁴ M. Binder, A. Nirschl, R. Zeisel, T. Hager, H.-J. Lugauer, M. Sabathil, D. Bougeard, J. Wagner, and B. Galler, *Appl. Phys. Lett.* **103**, 071108 (2013).
- ⁵ G.-B. Lin, D. Meyaard, J. Cho, E.F. Schubert, H. Shim, and C. Sone, *Appl. Phys. Lett.* **100**, 161106 (2012).
- ⁶ U. Ozgur, H. Liu, X. Li, X. Ni, and H. Morkoc, *IEEE Proc.* **98**, 1180 (2010).
- ⁷ J. Xie, X. Ni, Q. Fan, R. Shimada, U. Ozgur, and H. Morkoc, *Appl. Phys. Lett.* **93**, 121107 (2008).
- ⁸ J. Hader, J.V. Moloney, and S.W. Koch, *Appl. Phys. Lett.* **96**, 221106 (2010).
- ⁹ S. Hammersley, D. Watson-Parris, P. Dawson, M.J. Godfrey, T.J. Badcock, M.J. Kappers, C. McAleese, R.A. Oliver, and C.J. Humphreys, *J. Appl. Phys.* **111**, 083512 (2012).
- ¹⁰ N.I. Bochkareva, Y.T. Rebane, and Y.G. Shreter, *Appl. Phys. Lett.* **103**, 191101 (2013).
- ¹¹ E. Kioupakis, P. Rinke, K.T. Delaney, and C.G. Van de Walle, *Appl. Phys. Lett.* **98**, 161107 (2011).
- ¹² J. Hader, J.V. Moloney, and S.W. Koch, *Appl. Phys. Lett.* **99**, 181127 (2011).
- ¹³ J. Wang, L. Wang, W. Zhao, Z. Hao, and Y. Luo, *Appl. Phys. Lett.* **97**, 201112 (2010).
- ¹⁴ Y. Lin, Y. Zhang, Z. Liu, L. Su, J. Zhang, T. Wei, and Z. Chen, *J. Appl. Phys.* **115**, 023103 (2014).
- ¹⁵ J. Mickevičius, G. Tamulaitis, M. Shur, M. Shatalov, J. Yang, and R. Gaska, *Appl. Phys. Lett.* **103**, 011906 (2013).
- ¹⁶ J. Mickevičius, J. Jurkevičius, G. Tamulaitis, M.S. Shur, M. Shatalov, J. Yang, and R. Gaska, *Opt. Express* **22**, A491 (2014).
- ¹⁷ J. Mickevičius, J. Jurkevičius, A. Kadys, G. Tamulaitis, M.S. Shur, M. Shatalov, J. Yang, and R. Gaska, *J. Phys. D: Appl. Phys.* **48**, 275105 (2015).
- ¹⁸ T.H. Gfroerer, Y. Zhang, and M.W. Wanlass, *Appl. Phys. Lett.* **102**, 012114 (2013).
- ¹⁹ T. Malinauskas, K. Jarasiunas, M. Heuken, F. Scholz, and P. Bruckner, *Phys. Status Solidi C* **6**, S743 (2009).
- ²⁰ A. Pinos, V. Liuolia, S. Marcinkevičius, J. Yang, R. Gaska, and M.S. Shur, *J. Appl. Phys.* **109**, 113516 (2011).
- ²¹ S. Marcinkevičius, R. Jain, M. Shatalov, J. Yang, M. Shur, and R. Gaska, *Appl. Phys. Lett.* **105**, 241108 (2014).
- ²² S. Kim, J. Oh, J. Kang, D. Kim, J. Won, J.W. Kim, and H.-K. Cho, *J. Cryst. Growth* **262**, 7 (2004).